VOL. 12, NO. 8, APRIL 2017 ISSN 1819-6608
ARPN Journal of Engineering and Applied Sciences


www.arpnjournals.com

AERODYNAMICS CHARACTERISTICS AROUND SIMPLIFIED HIGH SPEED TRAIN MODEL UNDER THE EFFECT OF CROSSWINDS

Sufiah Mohd Salleh[1], Mohamed Sukri Mat Ali[1], Sheikh Ahmad Zaki Shaikh Salim[1], Izuan Amin Ishak[1], Masataka Shirakashi[1] and Sallehuddin Muhammad[2]
[1]Wind Engineering Laboratory, Malaysia-Japan International Institute of Technology, Universiti Teknologi Malaysia, Malaysia
[2]Department of Engineering, UTM Razak School of Engineering and Advanced Technology, Universiti Teknologi Malaysia, Malaysia
E-Mail: sufiahsalleh90@gmail.com

ABSTRACT

The aerodynamics problems of train commonly come when the flow pass through train body. The increasing speed of train to achieve highly technology demands has led to increase the forces and moments and increase sensitivity of train stability and may cause the train to overturn. In this paper, two prisms arranged in tandem represent a simplified model of high speed train are performed at different yaw angle ranging from 0˚ to 90˚ by using the unsteady Reynolds-Averaged Navier Stokes (URANS) equation combined with k-ω SST turbulence model. The Reynolds number is $3.14x10^5$based on height of the train and the free stream velocity. The aerodynamic quantities such as the side force, lift force and drag force coefficient show a similar trend where the forces increase with the yaw angle until a certain critical yaw angle before start to decrease till the yaw angle of 90˚. The flow structure around the train under the effect of crosswind is visualized. The vorticitiy start to form from the nose and slowly drifts away further towards the trailing edge. The two-dimensional mean streamlines on the cross-section of train at different yaw angle show that the size of vortex increase as the yaw angle increase. Time averaged pressure contour plotted on the cross section along x-axis show the variation of region between high pressure and low pressure region on the leeward and windward side of the train model that may cause train to overturn.

Keywords: crosswind, high speed train, URANS, k-ω SST turbulence model, flow structure.

INTRODUCTION

In the last three decades, a new trend of trains towards higher running speeds and light in weight has evolved in railway transportation. The speed of train may exceed 300km/h in regular operation and nearly comparable with the speed of light airplanes [1]. At these speeds, aerodynamic forces and moment are becoming more important for the running performance of the train. Strong crosswind may affect the running stability and riding comfort of the vehicle.

The increase of the aerodynamic forces and moments due to crosswind may influenced the train operating safety and the worst case may lead train to overturn. Recently, 29 wind-induced accidents were reported since the first high speed was introduced in Japan in 1872 [2]. Crosswinds stability of rail vehicles has gain the intention of a number of scholars mainly motivated by overturning accidents. The risk of crosswind that may cause train to overturn depends on the track infrastructure and vehicle aerodynamics [3]. Track infrastructure with tall viaduct and high embankment are exposed to strong crosswinds and sudden wind gust and led to increase the number of accident regarding to train overturning. On the other hands, aerodynamics plays an important role of train stability when exposed to strong crosswinds especially on the leading car. Leading car is the most sensitive part because it's exposed the highest aerodynamics forces and moment [4].

The study of train aerodynamic under the effect of crosswind is growing with the help various types of numerical simulation and wind tunnel. Hemida *et al.* (2005) was investigated the aerodynamic performance around simplified model of high speed train using LES. He found that the flow separation appear at the lateral edge near the nose of the train led to the creation of two vortices that start from the nose of the train [5]. Gawthorpe (1994) study the effect of yaw angle on the rolling moment of simplified train model. He found that at the yaw angle below 45˚, the inclined vortices found like a slender body and beyond 60˚, the flow on the leeside are resembles that behind a circular cylinder [6]. In 2006, Krajnovic investigated the flow structure around simplified model of ICE2 train for both 35^0 and 90^0 yaw angle. His work concluded that crosswind mainly shows transient at 90^0yaw angle and at the smaller yaw angle, the train is act like a slender body [7].

The objective of this paper is to investigate the aerodynamic characteristic of simplified model of high speed train subjected to crosswind using numerical method of unsteady RANS combined with k-ω SST turbulence model. This work using 2 prisms located in tandem orientation that represents the simplified model of train. Results of numerical method using the yaw angle ranging from 0˚ to 90˚ are summarized.

NUMERICAL SIMULATION

Governing reynolds averaged Navier-stokes equation

The flow around simplified high speed train model in this study is solved using unsteady Reynolds Averaged Navier-Stokes equations (URANS). The flow around the train has been considered as incompressible and is obtained by solving the incompressible form of the URANS equation combined with the help of turbulent

model [8]. The URANS equations are basically derived from the usual RANS equation, but the unsteady term has been maintained [9]. RANS equation is derived from two equations: continuity and Navier-Stokes equation for the incompressible flow as follows:

$$\frac{\partial u_i}{\partial x_i} = 0, \tag{1}$$

$$\rho \frac{\partial u_i}{\partial t} + \rho u_j \frac{\partial u_i}{\partial x_j} = -\frac{\partial p_i}{\partial x_j} + \frac{\partial}{\partial x_j}\left[\mu\left(\frac{\partial u_j}{\partial x_j} + \frac{\partial u_i}{\partial x_j}\right)\right] + \rho f_i \tag{2}$$

The velocity components and the pressure, p are nonlinear partial differential equations, which means that there is no analytical solution for the problem with arbitrary boundary conditions. The unsteady RANS equation is based on the decomposition of the flow parameters into time averaged and fluctuating component. The decomposed velocities and pressure into mean value and fluctuations are shown as follow

$$u_i = \bar{u}_i + u'_i \tag{3}$$

$$p_i = \bar{p}_i + p'_i \tag{4}$$

The Reynolds decomposed velocities and pressures are substitute into equation of continuity and Navier-Stokes equation by taking the time average parts and the time-averaged fluctuating parts are equal zero. The time averaged turbulent flow for continuity and RANS equation are shown below:

$$\frac{\partial \bar{u}_i}{\partial x_i} = 0, \tag{5}$$

$$\frac{\partial \bar{u}_i}{\partial t} + \bar{u}_j \frac{\partial \bar{u}_i}{\partial x_j} = -\frac{1}{\rho}\frac{\partial \bar{p}_i}{\partial x_i} + \frac{\partial}{\partial x_j}\left(\mu \frac{\partial \bar{u}_i}{\partial x_j} - \rho \overline{u'_i u'_j}\right) \tag{6}$$

Turbulence model

Turbulence model is a computational procedure to close the system of flow equation as derived before. In URANS simulation, the Reynolds stress tensor is resolved using an eddy-viscosity model based on the Boussinesq assumption as shown below:

$$-\rho \overline{U'_i U'_j} = \mu_t \left(\frac{\partial U_i}{\partial x_j} + \frac{\partial U_j}{\partial x_j} - \frac{2}{3}\frac{\partial U_k}{\partial x_k}\delta_{ij}\right) - \frac{2}{3}\rho k \delta_{ij} \tag{7}$$

Where K is the turbulent kinetic energy and ω is the specific dissipation rate. Both equations are solved using the following equation;

$$\frac{\partial k}{\partial t} + U_j \frac{\partial k}{\partial x_j} = P_k - \beta^* k\omega + \frac{\partial}{\partial x_j}\left[(v + \sigma_k v_T)\frac{\partial k}{\partial x_j}\right] \tag{8}$$

$$\frac{\partial \omega}{\partial t} + U_j \frac{\partial \omega}{\partial x_j} = \alpha S^2 - \beta \omega^2 + \frac{\partial}{\partial x_j}\left[(v + \sigma_\omega v_T)\frac{\partial \omega}{\partial x_j}\right] + 2(1 - F_1)\sigma_{\omega 2}\frac{1}{\omega}\frac{\partial k}{\partial x_i}\frac{\partial \omega}{\partial x_j} \tag{9}$$

where vT is the kinematic eddy viscosity and can be defined as follow;

$$v_T = \frac{a_1 k}{\max(a_1 \omega, SF_2)} \tag{10}$$

The following closure coefficient is used in this study;

$$F_2 = tanh\left[\left[max\left(\frac{2\sqrt{k}}{\beta^* \omega y}, \frac{500v}{y^2 \omega}\right)\right]^2\right] \tag{11}$$

Where y is the distance to the next surface,

$$P_k = min\left(\tau_{ij}\frac{\partial U_i}{\partial x_j}, 10\beta^* k\omega\right) \tag{12}$$

$$F_1 = \tanh\left\{\left\{min\left[max\left(\frac{\sqrt{k}}{\beta^* \omega y}, \frac{500v}{y^2 \omega}\right), \frac{4\sigma_{\omega 2} k}{CD_{k\omega} y^2}\right]\right\}^4\right\} \tag{13}$$

$$CD_{k\omega} = max\left(2\rho\sigma_{\omega 2}\frac{1}{\omega}\frac{\partial k}{\partial x_i}\frac{\partial \omega}{\partial x_i}, 10^{-10}\right) \tag{14}$$

$$\phi = \phi_1 F_1 + \phi_2(1 - F_1) \tag{15}$$

$$\alpha_1 = \frac{5}{9}, \alpha_2 = 0.44 \tag{16}$$

$$\beta_1 = \frac{3}{40}, \beta_2 = 0.0828, \beta^* = \frac{9}{100} \tag{17}$$

$$\sigma_{k1} = 0.85, \sigma_{k2} = 1, \sigma_{\omega 1} = 0.5, \sigma_{\omega 2} = 0.856 \tag{18}$$

2nd order backward scheme is used for temporal discretization, 3rd order QUICKV scheme is used for the convection term and 2nd order unbounded Gauss linear differencing scheme is used for the viscous term.

COMPUTATIONAL DOMAIN AND BOUNDARY CONDITION

Description of Model Geometry

The model used in this work consists of two identical prisms that representing the simplified model of high speed train. The prisms have a square cross-section with width of D, height is D and length is 4D. The carriage separation between the cars is chosen as 0.5D, the possible distance for the flow to reattach to the downstream car. The train model and definition of the coordinate system of simplified high speed train model is given in Figure-1:

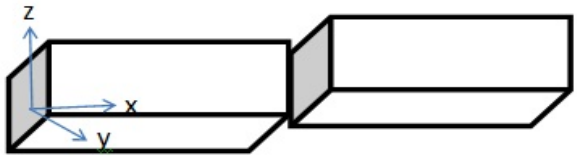

Figure-1. Train model with the coordinate system.

The non-dimensional aerodynamic side force, lift force and drag force presented in this work can be calculated as follow:

$$C_S = \frac{Side}{\frac{1}{2}\rho U_\infty^2 A}, \; C_L = \frac{Lift}{\frac{1}{2}\rho U_\infty^2 A}, \; C_D = \frac{Drag}{\frac{1}{2}\rho U_\infty^2 A}, \quad (19)$$

where ρ is the air density, is the free stream velocity and A is the prisms cross-sectional area. Lift, Side and Drag are the aerodynamic forces in the upward, sideward and backward to the trains.

Computational domain and boundary condition

Open source CFD software package of Open Foam software is used to simulate the problems. The different yaw angles are ranging from the yaw angle of 0˚ to 90˚ with the constant free stream velocity at inlet is applied. The computational domain used in this research is shown in Figure-2. Uniform free stream velocity and zero pressure gradients are applied at the inlet located at the front and side of the domain. The front inlet and side inlet are located 10D from the leading edge of the upstream body. The outlet is located 20D downstream from the trailing edge of the downstream body and 10D from the side of the model surface. Both sides are located at 10D from the train model and symmetrical boundary condition is applied for both sides.

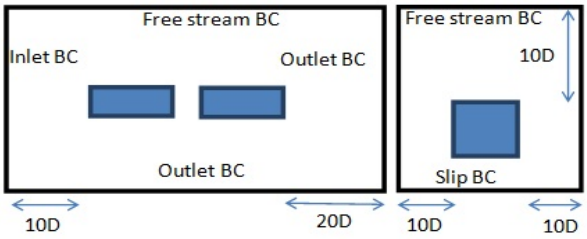

Figure-2. Sketch of computational domain view from top and front.

The cells in the computational domain are constructed using a structured non-uniform Cartesian mesh. Mesh refinement is applied on the train surface and its surrounding areas. The total generated mesh in this study is 5.86 million with the smallest cell size is 0.025D. Wall function is used for all the cases to reduce the computational cost by maintained the cell size near the surface [10]. The distance of the first cell layer to the model surface should be located within the requirements of y+. The Reynolds number used in this simulation is 3.14x105based on the height of the train's model and free stream velocity.

RESULT AND DISCUSSION

Aerodynamic forces

Figure-3 and Figure-4 below show the aerodynamic forces acting on the train model for the case of upstream and downstream body. As can be seen in Figure-3, the side force coefficients increase steadily with the yaw angle until the critical yaw angle of 75˚ before it start to decrease at the yaw angle of 90˚ because of the vortex breakdown occur at this critical yaw angle. Side force is caused by the pressure difference between windward side and leeward side of the train model. The pressure different on this two surfaces tend to cause train derailment when reaches the maximum side force. Lift forces and drag forces coefficients show the trend to increase steadily till the yaw angle of 30˚ before start to decrease. The lift forces coefficient decreases with the yaw angle is caused by the larger area of low pressure on the underneath surface compared to top surface of train model.

Figure-4 below shows the aerodynamic forces coefficient for side, lift and drag for the case of the downstream body. Side force coefficient increases steadily with the yaw angle. Like for the case of upstream body, lift force and drag force coefficient increases steadily with yaw angle before it start to decrease at critical yaw angle of 45˚ for lift force and 30˚ for drag force coefficient.

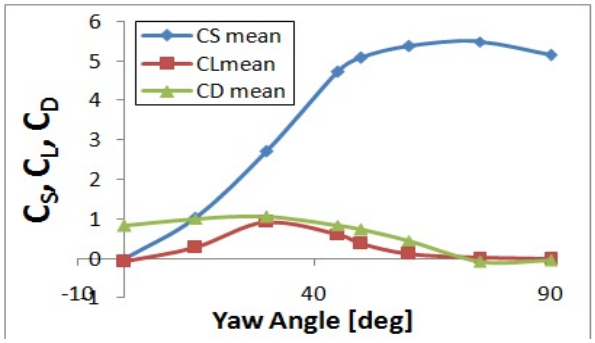

Figure-3. Aerodynamic force coefficient for upstream body.

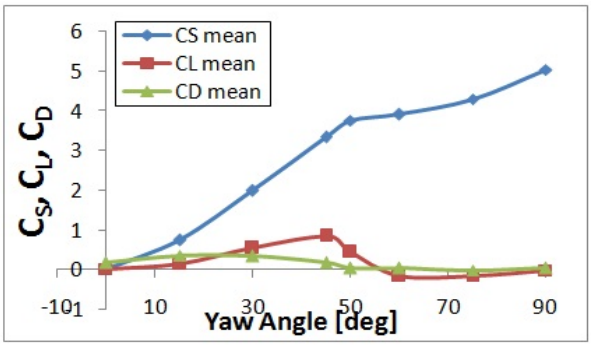

Figure-4. Aerodynamic force coefficient for downstream body.

Flow structure

The flow structure of two-dimensional streamline and pressure contour are used to explain more details the aerodynamic phenomena happen in Figure-4 and Figure-5. The train model is sliced into 4 different locations along x-axis as shown in Figure-5 below.

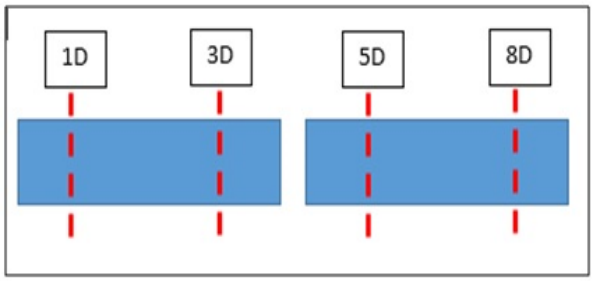

Figure-5. Train cross-section at different distance from the leading edge of train model.

Figure-6 above shows the vortex formation for the case of 30˚ yaw angle. Three vortices are clearly identified namely V1, V2 and V3. Vortex V1 keep increasing in size from the leading edge to the trailing edge of the train surface. For vortex V2, the vortex starts to drift away from the surface of train as further towards the trailing edge. At the distance of 1D from the nose, vortex V3 is attached at the top and side surface of train model and as the distance is further towards the trailing edge, the vortex is increase in size and remain attached only at the top surface of the train

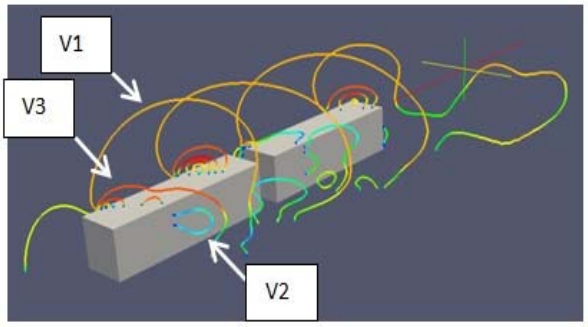

Figure-6. Vortex formation at different location along x-axis.

Figure-7 below shows the variation of vortex formation at distance 1D from the nose of the simplified high speed train model. As can be seen, flow separation takes place on both the lower and upper leeward edges. These vortices develop into larger size as the yaw angle increase. The presence of vortex on the leeward side formed the region of low pressure at the leeward (see Figure-8). As the vortex larger in size, the pressure is decreased and hence increase the side force on the leeward side.

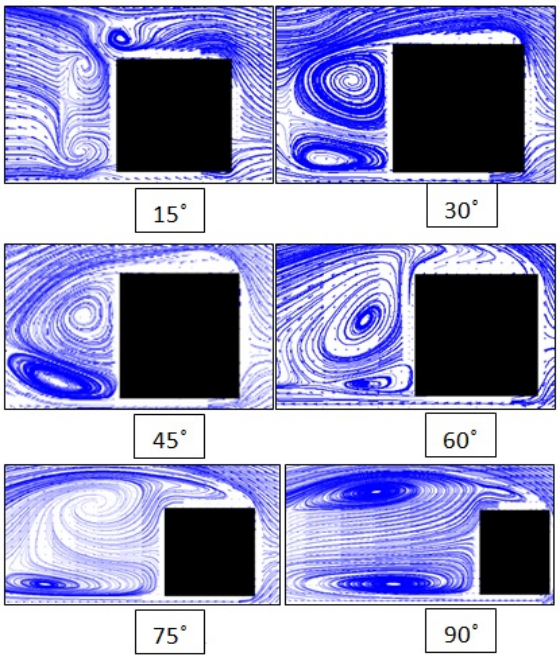

Figure-7. Mean streamlines along the train's cross section at the distance of 1D from the nose of the train.

Figure-8 shows the two-dimensional pressure contour at distance 1D from the nose of the train model at different yaw angle. All cases of yaw angle show the low region of pressure at the leeside of the model if compared to the windward side. At the yaw angle beyond 45˚, the pressure at the top surface of the model is lower than at the underneath surface this cause the lift force coefficient decreases with the yaw angle up to 45˚.

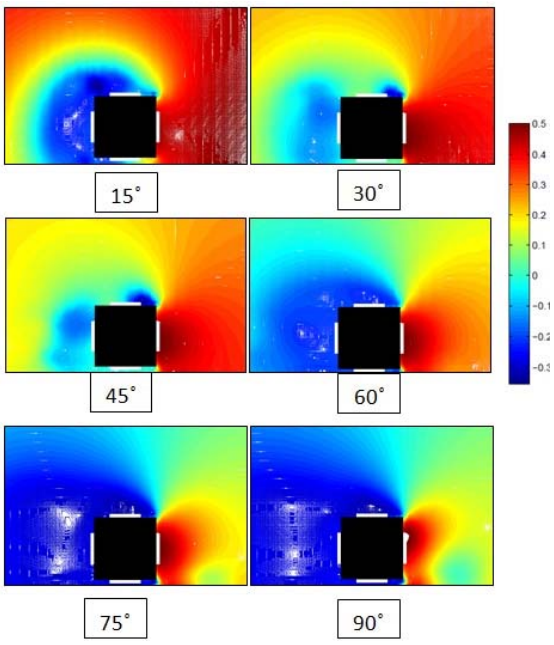

Figure-8. Pressure contour along train cross section at the distance of 1D from nose of the train model.

Figure-9 below shows the pressure distribution for upstream and downstream body around the top and bottom surfaces of the train model at the critical yaw angle of 75˚. At the nose region, downstream body has the higher pressure distribution compare to the upstream body because vortex formation produces on the upstream body is larger than the leading edge of downstream body. On the region behind train model, the wake produce at the trailing edge of the upstream body is larger than downstream body and this size is the major contribution of drag force [11].

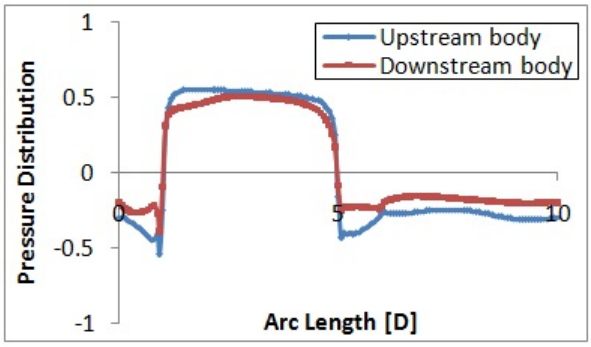

Figure-9. Pressure distribution at top and bottom surface of train model.

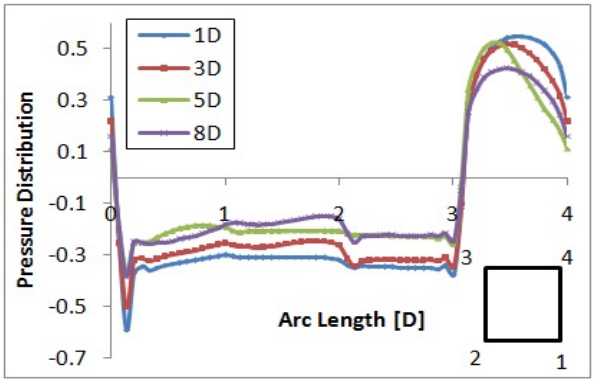

Figure-10. Pressure distribution along train's cross section at different distance from the nose of the train.

Figure-10 above shows the pressure distribution around the circumference of train at different cross section for the yaw angle of 75˚(see Figure-5). The graph shows that the pressure distribution does not change much along the train. This shows that the pressure distribution around the train model at higher yaw angles is independent with the axial position.

CONCLUSIONS

The flow around two prisms in tandem orientation have been simulated numerically using Unsteady Reynolds Navier-Stokes (URANS) equation combined with k-ω SST turbulence model for different case of yaw angles. URANS has the capability to produce flow structure and pressure distribution and has a good agreement with other scholar. The flow separation takes place on the lower and upper leeward surface and the size of vortex formation is depends on the yaw angle. The size of vortex is increased as the yaw angle is increased.

ACKNOWLEDGEMENTS

This research was financially supported by Malaysia Ministry of Higher Education (MOHE) under Research University Grant (RUG) project of Universiti Teknologi Malaysia (Vot No. Q.K130000.2643.09J79) and (Vot No. R.K130000.7843.4F479) also High Performance Computer (HPC) Universiti Teknologi Malaysia for the use of their supercomputer facilities. The first author also would like to acknowledge Universiti Teknologi Malaysia for the receipt of PhD. scholarship.

REFERENCES

[1] Raghunathan R. S., Kim H. D. and Toshiaki S. 2002. Aerodynamics of high-speed railway train. Progress in Aerospace sciences. 38(6): 469-514.

[2] Asress M. B, and Jelena S. 2014. Numerical investigation on the aerodynamic characteristics of high-speed train under turbulent crosswind."Journal of Modern Transportation. 22(4): 225-234.

[3] Elisa M. (Ed.) and Hoefener L. (Ed).2008. Aerodynamics in the open air (AOA), WP2 Cross Wind Issues. Final Report, DeuFrako Project.

[4] Simonovic A., Jelena S. and Slobodan S. 2014. Aerodynamic characteristics of high speed train under turbulent cross winds: A numerical investigation using unsteady-RANS method. FME Transactions. 42(1): 10-18.

[5] Hemida H. N. 2006. Large-eddy simulation of the flow around simplified high-speed trains under side wind conditions. Diss. Chalmers University of Technology.

[6] Gawthorpe R. G. 1994. Wind effects on ground transportation. Journal of Wind Engineering and Industrial Aerodynamics. 52: 73-92.

[7] Hemida H. N. and Siniša K. 2010. LES study of the influence of the nose shape and yaw angles on flow structures around trains. Journal of Wind Engineering and Industrial Aerodynamics 98(1): 34-46.

[8] Yang X., Jielong J. and Guangtian S. 2013. Preliminary study on streamlined design of longitudinal profile of high-speed train head shape. Procedia-Social and Behavioral Sciences. 96: 1469-1476.

[9] Menter F. R. 1994. Two-equation eddy-viscosity turbulence models for engineering applications. AIAA journal. 32(8): 1598-1605.

[10] Prime Z. 2014. Flow modelling and noise generation of interacting prisms. 20th AIAA/CEAS Aeroacoustics Conference.

[11] Guilmineau E. 2008. Computational study of flow around a simplified car body. Journal of wind engineering and industrial aerodynamic 96(6): 1207-1217.